Plasticity Initiation and Evolution during Nanoindentation of an Iron–3% Silicon Crystal

Ling Zhang[1] and Takahito Ohmura[1,2]
[1]Research Center for Strategic Materials, National Institute for Materials Science, 1-2-1 Sengen, Tsukuba, Ibaraki 305-0047, Japan
[2]Center for Elements Strategy Initiative for Structural Materials (ESISM), Kyoto University, Kyoto, 606-8501, Japan
(Received 4 June 2013; published 11 April 2014)

Our investigations confirm that the collective, avalanchelike dislocation nucleation and multiplication is responsible for the pop-in event in a body-centered-cubic Fe–3% Si single crystal. Dislocation was not observed prior to pop-in but was apparent after the event. We find that a transition from an initial stage dominated by discrete dislocation nucleation to subsequent continuum plasticity occurs just after the pop-in event as elastoplastic deformation ensues.

DOI: 10.1103/PhysRevLett.112.145504 PACS numbers: 62.25.−g

Nanoindentation has been widely used to investigate the fundamental aspects of mechanical behavior because of its ability to probe at the nanometer scale and therefore in defect-free sample volumes [1–4]. After several decades of research, the plasticity instability that is observed as a displacement excursion (load control) or load drop (displacement control) in metals, known as "pop-in" [4], has been agreed to be a process correlated with dislocation activities [5–11]. Several investigations have indicated the presence of mobile dislocations after pop-in [5,12–14], while recent observations using *in situ* nanoindentation in a transmission electron microscopy (TEM) have suggested that the plasticity occurs at much smaller forces than those observed at the first excursion detected in load control [10,15]. Whether the dislocation forms before or after the pop-in is of great scientific importance. Although there are many merits in this *in situ* technique, to understand the plasticity initiation and evolution in bulk material, the small-scale samples (such as nanopillars) have their limitations owing to the differences in the deformation conditions [16,17]. For example, the load-depth curve with only one large pop-in (as shown in Fig. 1) cannot be reproduced in the *in situ* deformation test [18,19] in which repeated pop-in events are commonly observed owing to the large free surface [20]. Figure 1 represents the load-depth curves of a body-centered-cubic (bcc) single crystal (Fe–3% Si) applied at two loads. This type of curve is common in bcc crystals, where only a single pronounced pop-in occurs [14,21,22]. Thus, investigations performed on the basis of bulk sample by nanoindentation need to be revisited. Until now, many attempts have been made to observe the dislocation structure around the indenter, but most studies have focused on measuring the plastic zone size for relatively large indentation impressions [23–26]. The purpose of our investigation was to understand the mechanism and role of pop-in behavior and to attempt to draw a general understanding of the initiation and evolution process of plasticity. By applying focused ion beam (FIB) milling, the systematic examination of the dislocation structure (right after the pop-in event) suggests that the transition arises from an initial stage, dominated by discrete dislocation nucleation, to subsequent continuum plasticity when elastoplastic deformation ensues. Importantly, dislocation was not found prior to the event, even at a stress level close to the pop-in threshold; hence, the presence of collective dislocations after pop-in was confirmed.

For our experiments, an electropolished (110)-oriented Fe–3% Si single crystal sample was used throughout. Load-control nanoindentation measurements were performed using a Hysitron Triboindenter with a Berkovich indenter (Hysitron, Inc., Minneapolis, MN). Both the loading and unloading rates of the indenter were set at 100 μN/s, without a holding segment. Since the initiation of the displacement burst is stochastic [27,28], the electropolished surface was indented with a load of 2 mN to obtain the average pop-in load (critical load, P_c). With an indenter tip radius of approximately 650 nm, fitted using the Hertz theory [29,30], as shown in Fig. 1, the average critical load was $P_c = 724 \pm 140$ μN. With this information, 11 groups of indentations with peak loads of 700, 750, and 800 μN were performed. The sites and configurations of the indents on the specimen surfaces were checked with an *in situ* scanning probe microscope (SPM) before and after the indentation measurements. The SPM measurements indicated a surface roughness of <3 nm. TEM (JEOL JEM-2010F) observation of the indent impressions was

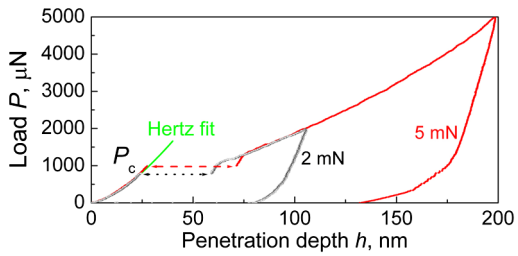

FIG. 1 (color online). Typical load-depth curves for Fe–3% Si single crystal.

conducted to check the dislocation character. The cross sectional and plane views of the indent impressions were prepared by using an FIB (JEOL JEM-9320). The sample surface was protected by carbon deposition before FIB milling. The TEM sample preparation method was similar to that of Ref. [31]. After lift-out, the sample slice was affixed to a TEM grid. The sample surface containing the indenter marks was placed perpendicular (cross section view sample) or parallel (plane-view sample) to the ion beam. The baseline for ion milling was set to the middle of the indenter impressions (cross section view) or a specific distance to the sample surface (plane view). The sample slice was thinned from both sides to a final thickness of ~100 nm to guarantee its transparency to the electron beam for imaging. The final beam current used was 10 pA with an accelerating voltage of 30 kV.

As a representative example, Fig. 2 illustrates a group of indentations, arranged in a 3×8 array, conducted at a maximum load of 750 μN. An SPM image of the sample before the FIB milling is shown in Fig. 2(a). Here the upper panel displays a schematic of the array in the presence and absence of residual impressions. Load-depth curves corresponding to the three indents numbered from 1 to 3 are plotted in Fig. 2(b) and can be divided into three types: type I exhibits no pop-in event (curve 2) and undergoes pure elastic loading and unloading. Type II has a pop-in load smaller than that of the applied load (curve 1); we refer to this phenomenon as "after-pop-in," which includes additional loading. Finally in type III, the critical load and applied load are almost equal (curve 3); we named this type "just-pop-in." The scanning TEM (STEM) image of the cross section is shown in Fig. 2(c). It is clear that no indent impression or dislocations are observed when the curves undergo pure elastic loading and unloading (curve 2). The pure elastic nature can be described by the Hertz contact theory as shown in Eq. (1) [29,30], where P is the applied load, R is the indenter tip radius, h is the displacement or depth, and E_r is the reduced modulus:

$$P = \frac{4}{3} E_r R^{1/2} h^{3/2}. \quad (1)$$

The deviation from the Hertz fit marks the onset of plastic deformation. The maximum shear stress, τ_{max}, needed to nucleate dislocations beneath the indenter can be given as Eq. (2) [30], where the reduced modulus E_r, measured from the unloading curve, is 201 GPa:

$$\tau_{max} = 0.18 \left(\frac{E_r}{R}\right)^{2/3} P^{1/3}. \quad (2)$$

At an average critical load P_c of 724 μN, τ_{max} can be estimated as 7.4 GPa, which is approximately one tenth of the shear modulus G (86 GPa) [14] and on the order of the theoretical strength ($G/2\pi \sim G/30$) [32]. Thus, dislocation nucleation and multiplication is expected at such a high stress. For our measurements, both indent impressions and dislocations were observed after a pop-in event, as shown in Figs. 2(a) and 2(c). The travel distance of the leading dislocation in the just-pop-in condition (curve 3) was ~1 μm. Heterogeneous dislocation nucleation assisted by surface roughness [33,34] or oxide film was neglected since the observed dislocations are merely located under the sample surface.

Figure 3 shows a plane-view sample with peak load of 750 μN, obtained at a depth ~200 nm from the sample surface. Figure 3(a) presents an example of the just-pop-in

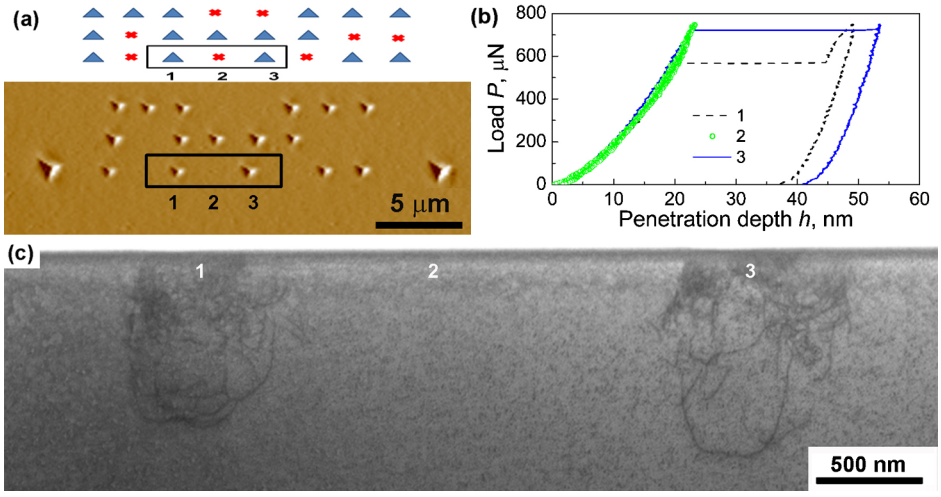

FIG. 2 (color online). Nanoindentation of the sample at a peak load of 750 μN. (a) SPM image of the indented group. The upper panel depicts the array with and without residual impressions. (b) Corresponding load-depth curves with after-pop-in (curve 1), no pop-in (curve 2), and just-pop-in (curve 3) events in the marked area. (c) The cross section of the marked area is observed by STEM and recorded on the [012] zone axis.

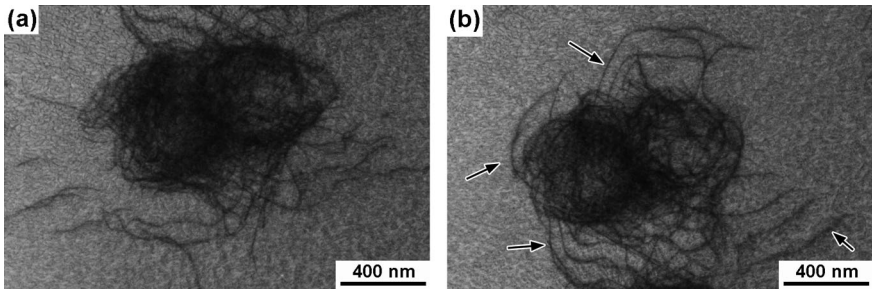

FIG. 3. A plane view of the sample with a peak load of 750 μN (obtained at a depth of ~200 nm from the sample surface). The STEM images were recorded close to the [210] zone axis. With (a) displaying the just-pop-in and (b) the after-pop-in conditions.

condition and Fig. 3(b) of the after-pop-in condition. The STEM images were obtained on the [210] zone axis. It is apparent that in Fig. 3(a), a local dislocated outer zone, with a highly dislocated core has already developed upon pop-in. The dislocation structures are similar in both the just-pop-in and after-pop-in conditions. However, a detailed comparison reveals that the dislocation distribution is random in the case of the just-pop-in condition [as shown in Fig. 2(c), curve 3 impression, and Fig. 3(a)], whereas in the after-pop-in impression, the dislocations tend to be somewhat parallel to each other or pile up [as shown in Fig. 2(c), curve 1 impression, and Fig. 3(b) indicated by arrows]. It is rationalized that the dislocations that are instantaneously formed under just-pop-in conditions can easily expand in various directions since there are no existing dislocations to serve as obstacles. The early formed dislocations are finally stopped by backstress or by simply running out of kinetic energy. Whereas for the after-pop-in conditions, previously formed dislocations can act as pre-existing dislocations; hence, the probability of dislocation-dislocation interactions increases, and pileup can be expected after further elastoplastic deformation. Furthermore, since the dislocation density under the indenter is significantly high after the pop-in event, the elastoplastic deformation (post-pop-in) can be assisted by the preexisting dislocations and shift to a continuum plasticity regime. This occurrence confirms the rationale of two load-depth curves overlapping with each other, as shown in Fig. 1. Here the depth is deeper than 75 nm, regardless of the differences in the pop-in loads.

The role of the pop-in event and a general understanding of plastic deformation connecting initial defect density can be understood on the basis of the schematic as shown in Fig. 4. Here, the thick solid line represents the relation between the stress necessary to initiate plastic deformation and dislocation density (ρ) [35,36] assuming that the dislocation nucleation or multiplication rate or dislocation mobility remains constant. During indentation of a clean crystalline metallic surface, if the initial dislocation density under the indenter is high enough (larger than ρ_c, in the part II regime), the preexisting dislocations can act as the source, and pop-in may not be necessary to sustain the strain rate; hence, the deformation undergoes a continuous plasticity.

In contrast, when the initial dislocation density under the indenter is smaller than the critical value ρ_c (part I regime), the initial loading of the load-depth (P-h) curve is purely elastic. Upon reaching a critical load P_c, the rapid onset of plastic deformation occurs. The stress necessary to initiate plastic deformation (point A in Fig. 4) decreases with increasing density of dislocations or defects. If the crystal is nearly perfect, stress levels close to the theoretical limit are necessary for dislocations to nucleate and multiply. If the density of defects under the indenter is $<\rho_c$, an increase in the initial defect density may increase the possibility of activating the existing dislocation source, therefore decreasing the shear stress needed to initiate plastic deformation. Thus, the maximum shear stress determined from the pop-in load increases with decreasing surface roughness [28] or prestraining [27,32] is observed. After the pop-in event, if the required dislocation density is created to sustain the plasticity, the deformation may fall into the continuum plasticity regime (from point A to B, as depicted in Fig. 4). To note that in the case of small-scale samples, even the local dislocation density after pop-in may instantaneously increase to a level that can be treated as in the continuum plasticity regime, for instance, a density close to but higher than ρ_c. The fast escaping of dislocations facilitated by large free surface may result in a dislocation starved state [20] and may require repeated pop-in events. The situation may be similar for the

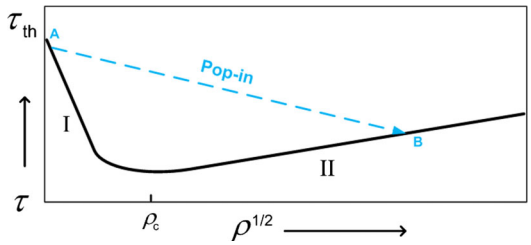

FIG. 4 (color online). Schematic illustration of the role of pop-in event. The thick solid line represents the relation between the stress and dislocation density. A transition via instantaneous pop-in event is illustrated with line A-B.

staircase-type deformation, as observed in face-centered-cubic Au [7] and Al [37] but requires further investigation to confirm this hypothesis.

As mentioned earlier, the travel distance of the leading dislocation is $\sim 1\ \mu$m in the just-pop-in condition. If the dislocations move at a constant rate, a dislocation velocity of approximately 2×10^{-4} m/s is necessary during the pop-in event (about 0.005 s in our case). Meanwhile, the average dislocation velocity (v) can be calculated by the following Orowan relation [38]:

$$v = \frac{\dot{\varepsilon}}{\rho b}. \tag{3}$$

For a symmetrical indenter tip, the strain rate ($\dot{\varepsilon}$) can be related to the penetration rate [39], where h is the penetration depth and t is time:

$$\dot{\varepsilon} = \frac{1}{h}\frac{dh}{dt}. \tag{4}$$

The dislocation density can be calculated by a line-intercept method, where the dislocation density is the number of points (N) divided by the total line length of random lines, L, multiplied by foil thickness, t_F, ($\rho = (N/Lt_F)$) [40]. For instance, the just-pop-in condition example in Fig. 2 shows that the local dislocation densities are $\sim 6 \times 10^{13}$ m^{-2} at the outer zone and $\sim 4 \times 10^{14}$ m^{-2} in the core area, respectively. The average strain rate during the pop-in event is estimated to be ~ 140 s^{-1}, whereas before or after pop-in, this is approximately 0.5 s^{-1}. By considering a strain rate of 140 s^{-1} and a dislocation density of 6×10^{13} m^{-2}, the dislocation velocity at the starting point of the pop-in event can be estimated as 9×10^{-3} m/s. Whereas, at the end of pop-in, the dislocation density reaches 4×10^{14} m^{-2} in the core area but the strain rate decreases to 0.5 s^{-1}; thus, the dislocation velocity can be calculated to be 5×10^{-6} m/s. If we compare the three dislocation velocities, it is evident that the pop-in event cannot be treated as an equilibrium process, where the dislocations move at a constant velocity. Thus, the most probable case is as follows: the stored elastic stain energy is considerably high just before plasticity commences. This leads to a collective dislocation avalanchelike behavior, as observed in small-scale samples [41,42] or sudden growth of the plastic zone in front of a crack tip [43] to release the energy that appears as a pop-in phenomenon in the load-depth curve. It is envisaged that the dislocations may nucleate and propagate from the position of maximum shear stress at a very large rate. Without obstacles (preexisting dislocations), the leading dislocations can penetrate into the sample from various directions and form the outer zone, resulting in a structure with low dislocation density. During the pop-in, continuous formation of dislocations may push the previously generated dislocations further into the sample; at the same time, backstress or exhaustion of elastic energy may block further nucleation of dislocations or drive dislocations to pile up close to the indenter tip. Therefore, the core area is formed to accommodate the plastic volume with higher dislocation density. Consequently, the dislocation nucleation or multiplication rate gradually decreases owing to exhaustion of the stored elastic energy and lattice friction.

It has previously been assumed that initially only a single dislocation forms with homogeneous character [7,13]. Then a heterogeneous multiplication event (such as dislocation sources similar to the Frank–Read source operating at lower stress, megapascal level [5]) results in a displacement burst. However, it is difficult to find prior experimental evidence to support or refute this proposed idea. First, the attentive TEM observations at the start of the pop-in event or at the end of the elastic loading reveal no single dislocation. Rather, our data suggest that when the critical condition for dislocation nucleation is satisfied, several dislocations might explosively nucleate and propagate from the same source (as evident from our *in situ* nanoindentation result [18]) within a short period, immediately after the formation of the so-called first dislocation and give rise to a pop-in event. Also, in bcc metals, due to the ease of cross slip, the very early-formed dislocations may cross slip to create multiplication sources.

It can be argued that although no single dislocation was found in Fig. 2(c) at position 2 (curve 2) it does not confirm that dislocations did not ever exist in the sample; it may be that the once-formed dislocations escape the surface during the unloading step. It is speculated that the phenomenon may happen under displacement control mode but is not the case for the load control mode. Let us assume that a dislocation embryo exists right before the unloading. It can expand to become a stable dislocation if we provide further stress; otherwise, it will retrieve when we remove the stress. As reported by Soer *et al.* [15], under the displacement control mode, the load may drop significantly (even to zero) during the unloading process and thus cannot provide the stress necessary to form a stable dislocation. However, as we found that the pop-in event can initiate and end within 0.005 s (the real time might be shorter based on the resolution of the nanoindentation machine). During the unloading, the stress under the indenter will decrease slightly within such a short period, which implies that if a dislocation embryo is present, the multiplication process will follow, and pop-in can be observed since the stress is still high enough.

On the basis of the present investigation, we confirm that the collective, avalanchelike dislocation nucleation and multiplication is responsible for the pop-in event in the bcc Fe-Si alloy. We observe no dislocations prior to pop-in compared to the vast number found in the postevent. These findings suggest that a transition occurs from an initial stage dominated by discrete dislocation nucleation to the

subsequent continuum plasticity immediately after the pop-in event, when elastoplastic deformation ensues.

This study was financially supported by the Ministry of Education, Science, Sports and Culture, Japan, through a Grant-in-Aid for Scientific Research (C), No. 23560852 (2011), by the CREST program of the Japan Science and Technology Agency (JST), and by the Elements Strategy Initiative for Structure Materials (ESISM).

[1] A. Gouldstone, H.-J. Koh, K.-Y. Zeng, A. E. Giannakopoulos, and S. Suresh, Acta Mater. **48**, 2277 (2000).
[2] L. Zhang, T. Ohmura, A. Shibata, and K. Tsuzaki, Mater. Sci. Eng. A **527**, 1869 (2010).
[3] T. Ohmura, K. Tsuzaki, N. Tsuji, and N. Kamikawa, J. Mater. Res. **19**, 347 (2004).
[4] A. Gouldstone, N. Chollacoop, M. Dao, J. Li, A. M. Minor, and Y.-L. Shen, Acta Mater. **55**, 4015 (2007).
[5] J. Li, K. J. Van Vliet, T. Zhu, S. Yip, and S. Suresh, Nature (London) **418**, 307 (2002).
[6] A. M. Minor, E. T. Lilleodden, E. A. Stach, and J. W. Morris, Jr, J. Mater. Res. **19**, 176 (2004).
[7] S. G. Corcoran, R. J. Colton, E. T. Lilleodden, and W. W. Gerberich, Phys. Rev. B **55**, R16057 (1997).
[8] W. A. Soer, K. E. Aifantis, and J. T. M. D. Hosson, Acta Mater. **53**, 4665 (2005).
[9] D. Lorenz, A. Zeckzer, U. Hilpert, P. Grau, H. Johansen, and H. S. Leipner, Phys. Rev. B **67**, 172101 (2003).
[10] A. M. Minor, S. A. S. Asif, Z. W. Shan, E. A. Stach, E. Cyrankowski, T. J. Wyrobek, and O. L. Warren, Nat. Mater. **5**, 697 (2006).
[11] W. W. Gerberich, J. C. Nelson, E. T. Lilleodden, P. Anderson, and J. T. Wyrobek, Acta Mater. **44**, 3585 (1996).
[12] S. A. S. Asif and J. B. Pethica, Philos. Mag. A **76**, 1105 (1997).
[13] C. Begau, A. Hartmaier, E. P. George, and G. M. Pharr, Acta Mater. **59**, 934 (2011).
[14] D. F. Bahr, D. E. Wilson, and D. A. Crowson, J. Mater. Res. **14**, 2269 (1999).
[15] W. A. Soer, J. T. M. D. Hosson, A. M. Minor, Z. Shan, S. A. S. Asif, and O. L. Warren, Appl. Phys. Lett. **90**, 181924 (2007).
[16] W. D. Nix, J. R. Greer, G. Feng, and E. T. Lilleodden, Thin Solid Films **515**, 3152 (2007).
[17] H. Bei, Y. F. Gao, S. Shim, E. P. George, and G. M. Pharr, Phys. Rev. B **77**, 060103 (2008).
[18] L. Zhang, T. Ohmura, K. Sekido, T. Hara, K. Nakajima, and K. Tsuzaki, Scr. Mater. **67**, 388 (2012).
[19] L. Zhang, T. Ohmura, K. Sekido, K. Nakajima, T. Hara, and K. Tsuzaki, Scr. Mater. **64**, 919 (2011).
[20] C. R. Weinberger and W. Cai, Proc. Natl. Acad. Sci. U.S.A. **105**, 14304 (2008).
[21] M. M. Biener, J. Biener, A. M. Hodge, and A. V. Hamza, Phys. Rev. B **76**, 165422 (2007).
[22] D. F. Bahr, D. E. Kramer, and W. W. Gerberich, Acta Mater. **46**, 3605 (1998).
[23] W. Zielinski, H. Huang, and W. W. Gerberich, J. Mater. Res. **8**, 1300 (1993).
[24] Y. L. Chiu and A. H. W. Ngan, Acta Mater. **50**, 2677 (2002).
[25] T. F. Page, W. C. Oliver, and C. J. McHargue, J. Mater. Res. **7**, 450 (1992).
[26] Y. Gaillard, C. Tromas, and J. Woirgard, Acta Mater. **51**, 1059 (2003).
[27] J. R. Morris, H. Bei, G. M. Pharr, and E. P. George, Phys. Rev. Lett. **106**, 165502 (2011).
[28] Y. Shibutani and A. Koyama, J. Mater. Res. **19**, 183 (2004).
[29] K. Durst, B. Backes, O. Franke, and M. Göken, Acta Mater. **54**, 2547 (2006).
[30] B. Yang and H. Vehoff, Acta Mater. **55**, 849 (2007).
[31] X. Meng-Burany and A. T. Alpas, Thin Solid Films **516**, 325 (2007).
[32] S. Shim, H. Bei, E. P. George, and G. M. Pharr, Scr. Mater. **59**, 1095 (2008).
[33] J. A. Zimmerman, C. L. Kelchner, P. A. Klein, J. C. Hamilton, and S. M. Foiles, Phys. Rev. Lett. **87**, 165507 (2001).
[34] J. D. Kiely, R. Q. Hwang, and J. E. Houston, Phys. Rev. Lett. **81**, 4424 (1998).
[35] L. Johnson and M. F. Ashby, Acta Metall. **16**, 219 (1968).
[36] E. T. Lilleodden and W. D. Nix, Acta Mater. **54**, 1583 (2006).
[37] Y. Shibutani, T. Tsuru, and A. Koyama, Acta Mater. **55**, 1813 (2007).
[38] W. W. Gerberich, S. K. Venkataraman, H. Huang, S. E. Harvey, and D. L. Kohlstedt, Acta Metall. Mater. **43**, 1569 (1995).
[39] C. L. Woodcock and D. F. Bahr, Scr. Mater. **43**, 783 (2000).
[40] D. M. Norfleet, D. M. Dimiduk, S. J. Polasik, M. D. Uchic, and M. J. Mills, Acta Mater. **56**, 2988 (2008).
[41] F. F. Csikor, C. Motz, D. Weygand, M. Zaiser, and S. Zapperi, Science **318**, 251 (2007).
[42] D. M. Dimiduk, C. Woodward, R. LeSar, and M. D. Uchic, Science **312**, 1188 (2006).
[43] G. Michot, Acta Mater. **59**, 3864 (2011).